Plant, Cell and Environment (2003) **26**, 1365–1371

A new method for vulnerability analysis of small xylem areas reveals that compression wood of Norway spruce has lower hydraulic safety than opposite wood

S. MAYR[1] & H. COCHARD[2]

[1]*Institut f. Botanik, Universität Innsbruck, Sternwartestr. 15, A-6020 Innsbruck, Austria and* [2]*UMR PIAF, Site INRA de Crouelle, Cedex 2, F-63039 Clermont-Ferrand France*

ABSTRACT

Compression wood is formed at the underside of conifer twigs to keep branches at their equilibrium position. It differs from opposite wood anatomically and subsequently in its mechanical and hydraulic properties. The specific hydraulic conductivity (k_s) and vulnerability to drought-induced embolism (loss of conductivity versus water potential ψ) in twigs of Norway spruce [*Picea abies* (L.) Karst.] were studied via cryo-scanning electron microscope observations, dye experiments and a newly developed 'Micro-Sperry' apparatus. This new technique enabled conductivity measurements in small xylem areas by insertion of syringe cannulas into twig samples. The hydraulic properties were related to anatomical parameters (tracheid diameter, wall thickness). Compression wood exhibited 79% lower k_s than opposite wood corresponding to smaller tracheid diameters. Vulnerability was higher in compression wood despite its narrower tracheids and thicker cell walls. The P_{50} (ψ at 50% loss of conductivity) was −3.6 MPa in opposite but only −3.2 MPa in compression wood. Low hydraulic efficiency and low hydraulic safety indicate that compression wood has primarily a mechanical function.

Key-words: *Picea abies*; cavitation; conductivity; conifer; embolism; hydraulic efficiency; opposite wood; wood anatomy.

INTRODUCTION

Evolution of the plant life form 'tree' corresponded with the evolution of special mechanical and hydraulic properties of its xylem. The structure of xylem differs within trees; for example, from pith to bark, from root to apex, from stem to branch and from nodes to internodes (e.g. Gartner 1995) due to different functional demands. This heterogeneity of wood provides – from a hydraulic point of view – an efficient and safe water support of main plant parts as well as the possibility to sacrifice less important parts during periods of drought stress (segmentation hypothesis; Zimmermann 1978). Enormous structural differences can be found even at a year ring level because of differences in early and latewood and because of reaction wood formation.

Reaction wood is developed as tension wood at the upper side of branches in hardwoods and as compression wood at the underside of conifer twigs upon gravity strain to keep stems or branches in their equilibrium position (Wilson & Archer 1977). Compression wood has wider annual rings, higher density due to thicker cell walls and narrower as well as shorter tracheids compared to opposite wood (e.g. Timell 1986; Lee & Eom 1988). Furthermore, its tracheids show higher lignin content and higher cellulose microfibril angles (e.g. Gorisek & Torelli 1999; Gindl 2002). Compression wood exhibits lower specific hydraulic conductivity (k_s); the lower branch halves of *Pseudotsuga menziesii* had only 68% of the k_s of upper branch halves (Spicer & Gartner 1998b). In another study (Spicer & Gartner 1998a), compression wood showed 32% of the k_s in opposite wood. In the same species, induction of compression wood formation by bending of young trees resulted in a reduction of k_s by 52% (Spicer & Gartner 2002). Although these studies well characterize the low hydraulic efficiency of compression wood, its hydraulic importance can only be estimated by considering hydraulic safety properties as well.

The hydraulic safety of xylem describes its specific resistance to embolism. In embolized xylem conduits, gas bubbles interrupt the transmission of negative pressure to the soil and block water transport ('cohesion theory', e.g. Boehm 1893; Dixon & Joly 1894; Richter 1972; Jackson & Grace 1994). Embolism is caused by freeze–thaw events or drought (e.g. Robson & Petty 1987; Robson, McHardy & Petty 1988; Sperry & Sullivan 1992; Tyree, Davis & Cochard 1994; Davis, Sperry & Hacke 1999; Hacke & Sperry 2001; Sperry & Robson 2001; Mayr, Schwienbacher & Bauer 2003). The term 'hydraulic safety' refers to drought-induced embolism hereafter and is characterized by vulnerability thresholds: at xylem-specific water poten-

Correspondence: Dr Stefan Mayr, Fax: + 43 512 507 2715; e-mail: stefan.mayr@uibk.ac.at

tial (ψ) thresholds, entry of gas bubbles from adjacent air-filled spaces occurs ('air-seeding'; Zimmermann 1983). The vulnerability thresholds are low in most conifers (e.g. Sperry & Tyree 1990; Cochard 1992; Jackson, Irvine & Grace 1995; Brodribb & Hill 1999; Mayr, Wolfschwenger & Bauer 2002; Mayr *et al*. 2003).

Sperry, Donelly & Tyree (1988) developed a method ('Sperry-apparatus') to measure embolism rates in xylem samples by determination of the increase in hydraulic conductivity after removal of enclosed air by repeated high pressure flushing (see also Chiu & Ewers 1993; Vogt 2001; Mayr *et al*. 2002). Vulnerability to drought-induced embolism can be determined, when embolism rates versus corresponding ψ are analysed. Nevertheless, with the original methodical design, only 'mean' embolism and vulnerability properties of whole segments can be investigated. Spicer & Gartner (1998a, b) therefore modified the sealing mechanism of this hydraulic system to measure conductivity and embolism rates of samples chiselled out of stems and branches (see also Domec & Gartner 2001; Spicer & Gartner 2001; Domec & Gartner 2002a, b; Spicer & Gartner 2002). In the present study, a newly developed measurement system based on Sperry's method was used, the 'Micro-Sperry apparatus'. It enabled quantitative analysis of flow rates in very small areas within xylem cross-sections of twigs. Thereby, syringe cannulas were inserted at the outflow end of xylem samples. Flow rates through xylem areas situated within the cannulas were measured with connected microlitre syringes.

Based on this method as well as on cryo-scanning electron microscope (SEM) observations and dye experiments, we compared drought-related vulnerability and specific hydraulic conductivity of compression and opposite wood in Norway spruce [*Picea abies* (L.) Karst.]. Hydraulic efficiency and safety properties were related to anatomical aspects.

MATERIALS AND METHODS

Plant material

Experiments were carried out on twigs of Norway spruce [*Picea abies* (L.) Karst.] harvested at 1300 m near Mt. Birgitz Köpfl, Tyrol in June and July 2002. Twigs (up to 1.5 m in length) were harvested, re-cut under water and transported to the laboratory. After saturation for 24 h, the twigs were dehydrated to various extents on the bench.

Water potential (ψ)

The value of ψ was measured in the laboratory with a pressure chamber (Model 1000 Pressure Chamber; PMS Instrument Company, Corvallis, OR, USA) using end segments (length <5 cm) of small side twigs. Measurements should be very close to ψ of the main branches xylem, because transpiration was extremely low.

Measurements of embolism rates and specific hydraulic conductivity (k_s)

Embolism rates (loss of conductivity) of xylem samples were measured according to the method described in Sperry *et al*. (1988) (see also Chiu & Ewers 1993; Vogt 2001; Mayr *et al*. 2002).

In the present study, the newly developed 'Micro-Sperry apparatus' (Fig. 1) was used: Xylem segments (about 25 mm in length and up to 10 mm in diameter) of twigs were prepared immersed in distilled water. After removal of the bark, the inflow end of samples was sealed in a water-filled silicone tube. At the outflow end, sharpened, water-filled steel cannulas [Valu-Set 0.6 × 20 mm (including silicone tubes with 1.5 mm inner diameter); Becton Dickinson Infusion Therapy Systems Inc., Sandy, UT, USA] were inserted 2–4 mm in compression and opposite wood, respectively. Each cannula was connected to a microlitre syringe (25 μL; Hamilton, Bonaduz, Switzerland) over a small water-filled silicone tube and a three-way valve. The latter allows the syringe water column to be set to a defined start point before each measurement: the water column is pushed forward or pulled back with a water-filled syringe (1 mL) connected to the three-way valve. Flow was calculated from volume changes within the syringe capillaries during the measurement time (usually between 2 and 5 min). Measurement pressure was set to 4 kPa (controlled via a 0.4 m glass capillary). Flushing (removal of embolism at 0.13 MPa, 20 min) and conductivity measurements were performed with distilled, filtered (0.22 μm) and degassed water containing 0.005% (v/v) 'Micropur' (Katadyn Products Inc., Wallisellen, Switzerland) to prevent microbial growth (Sperry *et al*. 1988). Flushing was repeated until measurements showed no further increase in conductivity. The percentage loss of conductivity was calculated from the ratio of initial to maximal conductivity.

The specific hydraulic conductivity k_s was calculated from fully hydrated samples as in Eqn 1:

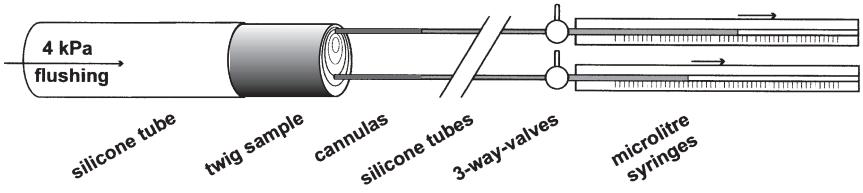

Figure 1. Micro-Sperry apparatus. At the inflow end, xylem samples were sealed in silicone tubes connected to a reservoir with filtered and degassed water. At the outflow end of samples, sharpened syringe cannulas were inserted in compression and opposite wood and connected to microlitre syringes over three-way valves. Before and after flushing, flow rate at 4 kPa was determined volumetrically.

$$k_s = Q \cdot l/(A_c \cdot \Delta P) \quad (1)$$

where k_s is in $m^2\ s^{-1}\ MPa^{-1}$, Q is the volume flow rate ($m^3\ s^{-1}$), l is the length of the segment (m), A_c is the cross-sectional area situated inside the cannula (m^2, see anatomical measurements), and ΔP is the pressure difference between the segment ends (MPa). Calculations were corrected to 20 °C to account for changes in fluid viscosity with temperature.

Vulnerability curves

Vulnerability curves were obtained by plotting percentage loss of hydraulic conductivity versus ψ. Curves were fitted with the exponential sigmoidal equation (Eqn 2) given in Pammenter & Vander Willigen (1998):

$$PLC = 100/(1 + \exp[a(\psi - b)]) \quad (2)$$

where PLC is the percentage loss of conductivity, ψ is the corresponding water potential (MPa) and a and b are constants. Measurement series with a maximal flow rate below 0.01 $\mu L\ s^{-1}$ were not considered for vulnerability analysis.

Dye experiments

(A) Micro-Sperry control experiment

This approach should demonstrate the flow distribution within the xylem cross-sectional area, which is relevant for flow measurements with the Micro-Sperry method. The inflow end of xylem samples was connected to a specially prepared silicone tube (Fig. 2): A tube fitting to the circumference of the sample contained two small tubes filled with dye solution [Phloxine B; Sigma Chemical CO., St. Louis, MO, USA; 2% (w/v)]. First, sharpened cannulas connected to the small tubes were inserted in compression and opposite wood at the sample inflow end. Second, the whole sample was sealed to the big tube (filled with distilled water). This tube was connected to a water reservoir, the small tubes to a Phloxine B reservoir, both mounted 40 cm above the outflow end of the sample (4 kPa pressure gradient over the whole xylem cross-section). When dye solution appeared at the outflow end of samples the reservoirs were disconnected. Samples were cut every 2 cm and pictures of cross-sections were taken.

This experiment indicated that flow through xylem occurred nearly completely in the axial direction of the samples (Fig. 2), as previously reported by other authors (e.g. Kubler 1991). The radial flow of water was minimal at the pressure gradient used in this experiment. Due to lower specific hydraulic conductivity, staining in compression wood did not proceed through the whole sample before the experiment was stopped. We conclude that the Micro-Sperry apparatus measures flow rates through axial tracheid pathways ending within inserted cannulas.

(B) Vulnerability experiment

From twigs that had been dehydrated to various extents, segments about 2 cm long were sealed in a silicone tube connected to a reservoir with 2% (w/v) Phloxine B solution. After staining (4 kPa, 5 min), cross-sections of samples were prepared.

Cryo-SEM observations

From dehydrated twigs (0, 2.7, 3.3, 3.7 and 5.0 MPa) compression and opposite wood samples (length 2 cm, diameter <2 mm) were prepared while immersed in distilled water. Samples were frozen and stored in liquid nitrogen until use for Cryo-SEM analysis.

Samples (still immersed in liquid nitrogen) were fixed in about 3 mm deep holes made in an aluminium bar screwed on the specimen holder. Next, samples were fractured with pliers and rapidly transferred to the cryo-preparation chamber of the microscope held at –150 °C (model CT 1000, Hexland; Oxford Instruments Ltd, Oxford, UK). After vacuum was created in the chamber, samples were moved to the sample stage (–150 °C) in the SEM column (model SEM 505; Philips, Eindhoven, The Netherlands). Samples were observed uncoated at 5.2 kV. Surface etching was achieved by setting the stage temperature to –80 °C for several minutes.

Anatomical measurements

Anatomical measurements were performed on twig samples previously used for conductivity measurements. Cross-

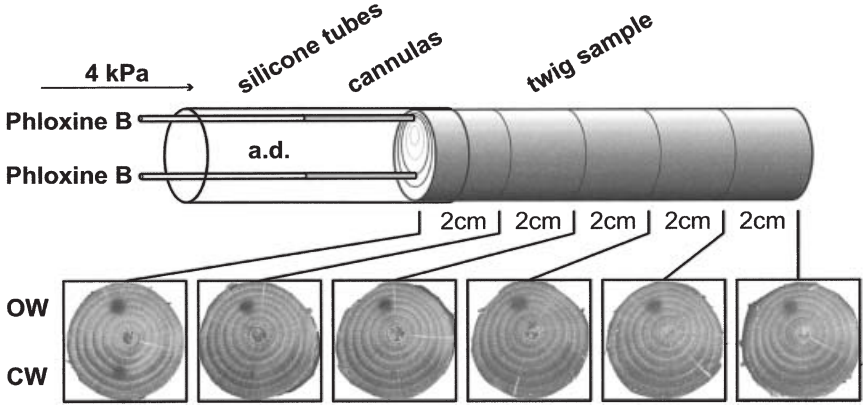

Figure 2. Micro-Sperry control experiment. Sharpened syringe cannulas were inserted in compression (CW) and opposite (OW) wood at the inflow end of a 10-cm long xylem sample. Cannulas were connected to a reservoir with Phloxine B dye solution. Additionally, the whole sample was sealed in a silicone tube connected to a reservoir with distilled, filtered and degassed water (a. d). After flow of the solution through the sample at 4 kPa, reservoirs were disconnected and sample cross-sections were prepared every 2 cm.

sections of xylem areas situated inside the cannulas during conductivity measurements, were prepared. From these small xylem discs, tracheid cross-sectional areas (lumen) were determined microscopically (Olympus BX50; Olympus Austria Corp., Vienna, Austria; 200-fold magnification) with an automated image analysis system (Optimas 6.0; Optimas Corporation, Washington, DC, USA). Mean tracheid lumen span (termed tracheid diameter in the following) was calculated assuming rectangular tracheid shape. Mean hydraulic diameter d_h was determined by re-weighting diameter distribution according to the Hagen–Poiseuille law (Zimmermann 1983) as described in Kolb & Sperry (1999). From tracheids which averaged within ±0.5 μm of d_h, span (b) and corresponding thickness of the double wall (t) was measured. According to Hacke *et al.* (2001), the ratio $(t/b)_h^2$ was calculated. The whole area of prepared xylem discs (A_c) was also measured for the calculation of k_s.

Number of samples, statistics

Vulnerability was analysed from 34 (compression wood) and 58 (opposite wood) embolism measurements with the Micro-Sperry apparatus. The value of ψ was measured on at least three parallel samples of each dehydrated twig. The value of k_s of compression and opposite wood was determined from 15 twig samples. Anatomical measurements were carried out on corresponding 15 cross-sectional discs (xylem area previously situated in cannulas during Micro-Sperry measurements) of compression and opposite wood, respectively. The $(t/b)_h^2$ ratio was determined from 55 (compression wood) and 50 (opposite wood) tracheids. Values are given as mean ± standard error. Differences were tested at 1% probability level with Student's t-test after checking for normal distribution and variance of the data or with a Mann–Whitney test (tracheid diameter distribution).

RESULTS

Anatomy

Compression wood exhibited significantly narrower tracheids than opposite wood (Table 1, Fig. 3). Within each twig sample, mean tracheid diameter of compression wood was 70.24 ± 4.2% and d_h was 81.0 ± 4.2% that of opposite wood. Because of smaller tracheid diameters and thicker cell walls the $(t/b)_h^2$ ratio was significantly higher in compression wood (Table 1).

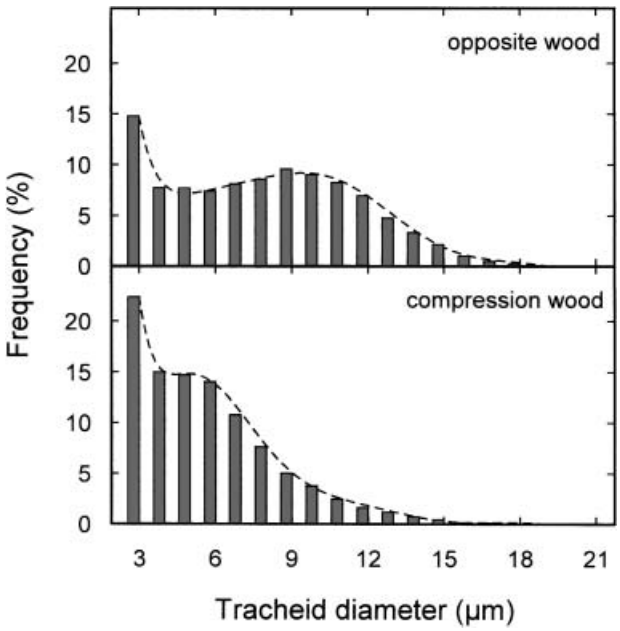

Figure 3. Frequency distribution of tracheid cross-sectional diameters in compression and opposite wood. Diameters of tracheid lumen were determined from xylem cross-sectional discs situated inside the cannulas during Micro-Sperry measurements. Frequency distributions differ significantly at $P \leq 0.01$.

Specific hydraulic conductivity (k_s)

Compression wood exhibited a significantly lower k_s than opposite wood (Table 2). Within each twig sample, k_s of compression wood was only 20.7 ± 3.9% that of opposite wood.

Vulnerability to drought-induced embolism

Quantitative analysis of vulnerability to drought-induced embolism via Micro-Sperry apparatus revealed compression wood to reach 10% loss of conductivity (P_{10}) as well as 50% loss of conductivity (P_{50}) at significantly less negative ψ (Fig. 4, Table 2). Parameter a (curve slope, Pammenter &

Table 1. Anatomical parameters of compression and opposite wood in twigs of Norway spruce

	Mean diameter (μm)	Maximum diameter (μm)	d_h (μm)	t (μm)	$(t/b)_h^2$
Compression wood	5.29 ± 0.02[a]	18.96	10.49 ± 0.01[a]	6.26 ± 0.26[a]	0.393 ± 0.03[a]
Opposite wood	7.48 ± 0.03[b]	21.23	12.21 ± 0.01[b]	3.64 ± 0.15[b]	0.097 ± 0.01[b]

Mean tracheid lumen diameter (mean diameter), maximum diameter, mean hydraulic diameter d_h (hydraulic diameter; Kolb & Sperry 1999) and wall thickness t are in μm. Parameter $(t/b)_h^2$ was calculated from the wall thickness t and the conduit wall span b according to Hacke *et al.* (2001). Values of each column not followed by the same letter differ significantly at $P \leq 0.01$ (Student's t-test). Values are mean ± SE.

Table 2. Hydraulic parameters of compression and opposite wood in twigs of Norway spruce

	k_s ($m^2\ s^{-1}\ MPa^{-1}\ 10^{-4}$)	Parameter *a*	P_{50} (MPa)	P_{10} (MPa)
Compression wood	1.67 ± 0.34^a	1.90 ± 0.30^a	-3.18 ± 0.08^a	-2.02 ± 0.26^a
Opposite wood	8.46 ± 0.91^b	3.46 ± 0.49^b	-3.57 ± 0.04^b	-2.93 ± 0.13^b

Specific hydraulic conductivity k_s is in $m^2\ s^{-1}\ MPa^{-1} \times 10^{-4}$, Vulnerability curve parameters according to Pammenter & Vander Willigen (1998): Parameter a is related to the curve slope, parameter *b* (50% loss of conductivity, P_{50}) and the upper vulnerability threshold (10% loss of conductivity, P_{10}) are given in MPa. Values of each column not followed by the same letter differ significantly at $P \leq 0.01$ (Student's *t*-test). values are mean ± SE.

Vander Willigen 1998) showed a steeper increase of embolism rates with decreasing ψ in opposite wood.

Similar results were obtained by cryo-SEM observations (Fig. 5) of twigs dehydrated to different ψ. At –3.3 MPa, several embolized tracheids were found in compression but not in opposite wood. At –3.7 MPa, compression wood was nearly fully embolized, whereas opposite wood still showed mainly water-filled conduits. Due to helical cavities (Lee & Eom 1988), air content of compression wood tracheids was sometimes difficult to recognize (e.g. Fig. 5; 3.7 MPa).

Vulnerability properties could also be seen from dye experiments. Figure 6 shows a cross-section of a twig dehydrated to –3.5 bar. In compression wood, embolized fields appeared especially in earlywood areas (Fig. 6B), whereas opposite wood was completely stained.

DISCUSSION

Anatomical investigations showed compression wood to have smaller tracheids (Fig. 3, Table 1) and thicker cell walls; parameters which we expected to correlate with hydraulic properties.

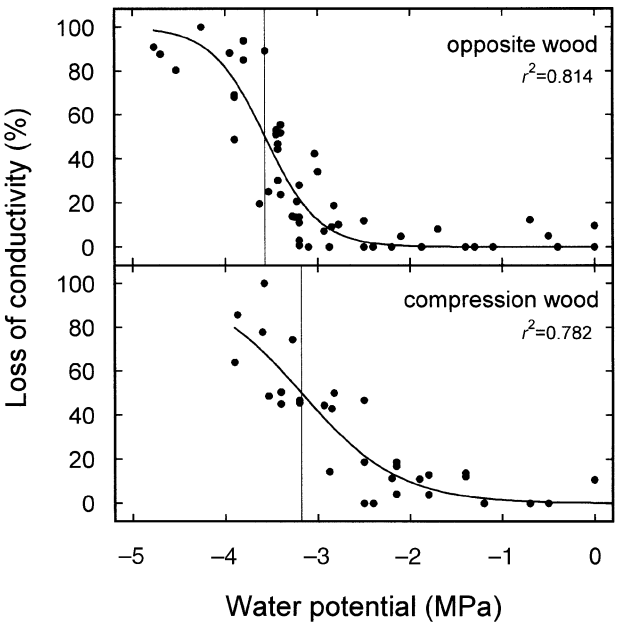

Figure 4. Vulnerability curves (loss of conductivity versus water potential) of compression and opposite wood. Curves were fitted by the equation described in Pammenter & Vander Willigen (1998). P_{50} is indicated by vertical lines.

Lower hydraulic efficiency of compression wood has already been demonstrated in *Pseudotsuga menziesii* by Spicer & Gartner (1998a,b) and Spicer & Gartner (2002). In the present study, differences in k_s were even higher (79%, Table 2), because the new method allowed measurements in the centre of compression and opposite wood, whereas previous methodical approaches measured flow in branch halves (Spicer & Gartner 1998b) or quarters (Spicer & Gartner 1998a). Furthermore, properties may also differ with species and gravity or wind loads of branches. The reduced k_s in compression wood was not solely caused by its smaller tracheid lumen because d_h was only 14% smaller than in opposite wood (Table 1). The discrepancy between k_s and d_h can be explained by the lower portion of conducting area in compression wood due to higher amounts of intercellular spaces and thicker cell walls. Within the xylem discs analysed, cumulative tracheid lumen was only 9.4% of the whole area in compression but 18.0% in opposite wood. Furthermore, shorter tracheids and smaller pit apertures (Timell 1986; Lee & Eom 1988; Spicer & Gartner 1998b) may contribute to the low k_s of compression wood.

Hydraulic safety is correlated with wood density, when angiosperm and conifer species are compared (Hacke *et al.* 2001; see also Hacke & Sperry 2001). The best correlation was found with factor $(t/b)_h^2$ which relates span *b* and wall thickness *t* of conduits. Calculating this factor for opposite and compression wood (Table 1), one would expect the latter to be much more resistant to drought-induced embolism. In contrast, Micro-Sperry measurements (Table 2, Fig. 4), cryo-SEM observations (Fig. 5) and dye experiments (Fig. 6A) revealed compression wood to have even lower hydraulic safety. Embolism occurred already at about 0.9 MPa less negative ψ (P_{10}) than in opposite wood. Compression wood was more and opposite wood less vulnerable when compared with the P_{50} of whole twigs (–3.39 MPa; Mayr *et al.* 2002). It has to be considered that vulnerability curves measured on whole twig samples primarily reflect the hydraulic properties of xylem parts with high conductivity, whereas the properties of the remaining wood may be masked. Spicer & Gartner (1998a) demonstrated that lateral wood has a higher k_s than compression and opposite wood. According to this, factor $(t/b)_h^2$ may be well correlated to vulnerability properties of whole twigs at an interspecific level, because it is the highly conductive xylem

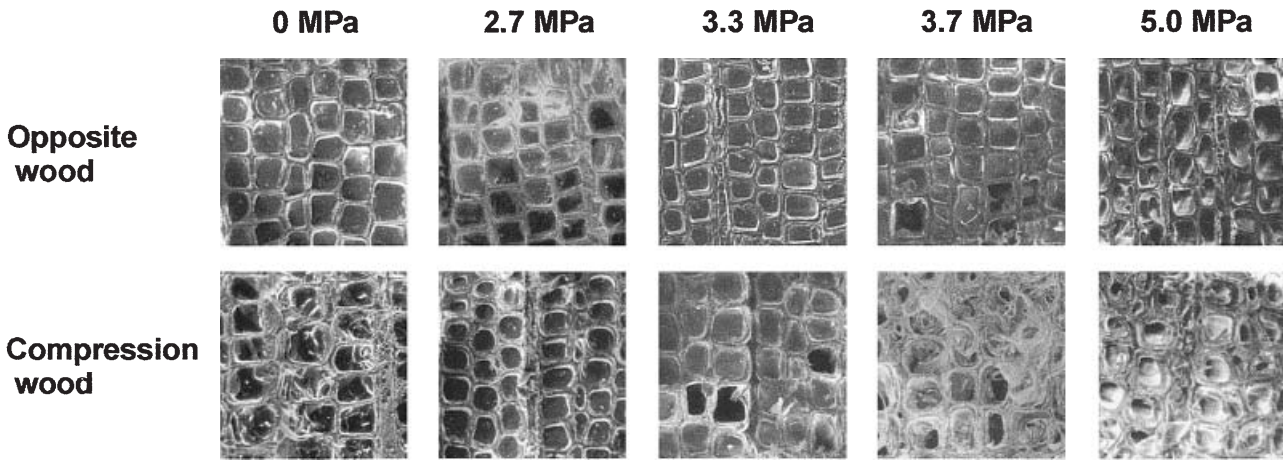

Figure 5. Cryo-SEM observations of compression and opposite wood. Earlywood of xylem samples dehydrated to various ψ was studied with the cryo-SEM. Corresponding compression and opposite samples were prepared for each twig sample, respectively. Tracheids, dark and unstructured in the lumen are embolized. Photos show 100×100 μm.

parts that are always compared. Therefore, $(t/b)_h^2$ of opposite wood also fits to the correlation found by Hacke *et al.* (2001). In contrast, the presented results indicate that $(t/b)_h^2$ cannot reflect hydraulic properties of compression and opposite wood within branches. Variation of xylem properties at this scale obviously exceed differences of (mean) properties between species (e.g. Gartner 1995).

Domec & Gartner (2002) have already suggested compression wood to be more vulnerable because it contains higher amounts of latewood. Latewood showed less hydraulic safety probably due to its pit anatomy, which does not enable a sufficient seal of the margo. Nevertheless, despite its high upper vulnerability threshold, latewood was reported to still show some conductivity at low ψ (Domec & Gartner 2002). This corresponds to the lower slope of the vulnerability curve of compression wood (Table 2, Fig. 4). In cryo-SEM observations, some water-filled fields in latewood were found (data not shown). Additionally in dye experiments, we observed latewood near the borders of year rings to exhibit some staining, even when the main parts of the late and earlywood were already embolized (Fig. 6B). Within earlywood, tracheids near the year ring borders seem to cavitate last, which led (at –3.5 MPa) to an unstained band in the middle of each year ring (Fig. 6B). This indicates that embolism started in early latewood, followed by the earlywood (first in late then in early earlywood), while late latewood stayed functional down to extreme ψ. Sperry & Tyree (1990) presented photos of conifer cross-sections, which also showed some (Safranan) staining in latewood at the year ring border, whereas all other areas were embolized. These photographss also indicated more embolism in compression (oriented to the upper side) than in opposite wood. Future investigations probably will give further insight into differences between early and latewood within compression, opposite and lateral wood.

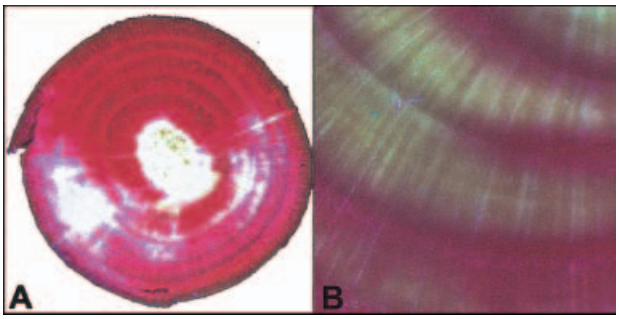

Figure 6. Dye perfusion. A xylem sample dehydrated to –3.5 MPa was stained via Phloxine B perfusion at 4 kPa. (a) Distribution of embolized areas (white-coloured areas in the compression wood, which is situated at the lower side) in the cross-section of the whole twig. (b) Distribution of embolized areas within the compression wood. Photograph (a) shows 10×10 mm, (b) shows 2×2 mm.

There are other anatomical aspects, which may contribute to the low hydraulic safety of compression wood: the high amount of intercellular spaces caused by the rounded shape of tracheids (Lee & Eom 1988) could increase the probability of air-seeding processes. Spicer & Gartner (1998b) reported a lower water content and higher specific gravity of lower branch halves and suggested that this was in part due to air occupying intercellular spaces. The most important aspect determining resistance to air seeding processes is the pit architecture, which differs in compression and opposite wood as well as in early and latewood (reviewed in Timell 1986). Furthermore, the higher lignin fraction of compression wood may influence its vulnerability.

Tracheids of conifer xylem have both mechanical and hydraulic function. Low hydraulic efficiency and low hydraulic safety of compression wood indicate a primarily mechanical function of this tissue. The physiological benefit, if there is any, of increased vulnerability in compression wood remains unclear. Nevertheless, at low ψ, latewood within compression wood could be important in order to maintain minimal conductivity.

ACKNOWLEDGMENTS

This study was supported by the University Innsbruck (Förderungsbeiträge) and by the Austrian 'Fonds zur Förderung der wissenschaftlichen Forschung'. We wish to thank Birgit Dämon, University Innsbruck and Sabine Rosner, Universität für Bodenkultur, Vienna for helpful assistance and Johanna Wagner, University Innsbruck for providing the equipment for anatomical analysis.

REFERENCES

Boehm H. (1893) Capillarität und Saftsteigen. *Berichte der Deutschen Botanischen Gesellschaft* **11,** 203–212.

Brodribb T. & Hill R.S. (1999) The importance of xylem constraints in the distribution of conifer species. *New Phytologist* **143,** 365–372.

Chiu S. & Ewers F.W. (1993) The effect of segment length on conductance measurements in *Lonicera fragrantissima*. *Journal of Experimental Botany* **44,** 175–181.

Cochard H. (1992) Vulnerability of several conifers to air embolism. *Tree Physiology* **11,** 73–83.

Davis S.D., Sperry J.S. & Hacke U.G. (1999) The relationship between xylem conduit diameter and cavitation caused by freezing. *American Journal of Botany* **86,** 1367–1372.

Dixon H.H. & Joly J. (1894) On the ascent of sap. *Proceedings of the Royal Society London* **57,** 3–5.

Domec J.C. & Gartner B.L. (2001) Cavitation and water storage capacity in bole xylem segments of mature and young Douglas-fir trees. *Trees* **15,** 204–214.

Domec J.C. & Gartner B.L. (2002a) Age- and position-related changes in hydraulic versus mechanical dysfunction of xylem: inferring the design criteria for Douglas-fir wood structure. *Tree Physiology* **22,** 91–104.

Domec J.C. & Gartner B.L. (2002b) How do water transport and water storage differ in coniferous earlywood and latewood? *Journal of Experimental Botany* **53,** 2369–2379.

Gartner B.L. (1995) Patterns of xylem variation within a tree and their hydraulic and mechanical consequences. In *Plant Stems: Physiology and Functional Morphology* (ed. H.A. Mooney), pp. 125–149. Academic Press, New York, USA.

Gindl W. (2002) Comparing mechanical properties of normal and compression wood in Norway spruce: the role of lignin in compression parallel to the grain. *Holzforschung* **56,** 395–401.

Gorisek Z. & Torelli N. (1999) Microfibril angle in juvenile, adult and compression wood of spruce and silver fir. *Phyton* **39,** 129–132.

Hacke U.G. & Sperry J.S. (2001) Functional and ecological xylem anatomy. *Perspectives in Plant Ecology, Evolution and Systematics* **4,** 97–115.

Hacke U.G., Sperry J.S., Pockman W.T., Davis S.D. & McCulloh K.A. (2001) Trends in wood density and structure are linked to prevention of xylem implosion by negative pressure. *Oecologia* **126,** 457–461.

Jackson G.E. & Grace J. (1994) Cavitation and water transport in trees. *Endeavour* **18,** 50–54.

Jackson G.E., Irvine J. & Grace J. (1995) Xylem cavitation in Scots pine and Sitka spruce saplings during water stress. *Tree Physiology* **15,** 783–790.

Kolb K.J. & Sperry J.S. (1999) Differences in drought adaptation between subspecies of sagebrush (*Artemisia tridentata*). *Ecology* **80,** 2373–2384.

Kubler H. (1991) Function of spiral grain in trees. *Trees* **5,** 125–135.

Lee P.W. & Eom Y.G. (1988) Anatomical comparison between compression wood and opposite wood in a branch of Korean pine (*Pinus koraiensis*). *IAWA Bulletin* **9,** 275–284.

Mayr S., Schwienbacher F. & Bauer H. (2003) Winter at the alpine timberline: why does embolism occur in Norway spruce but not in stone pine? *Plant Physiology* **131,** 1–13.

Mayr S., Wolfschwenger M. & Bauer H. (2002) Winter-drought induced embolism in Norway spruce (*Picea abies*) at the Alpine timberline. *Physiologia Plantarum* **115,** 74–80.

Pammenter N.W. & Vander Willigen C. (1998) A mathematical and statistical analysis of the curves illustrating vulnerability of xylem to cavitation. *Tree Physiology* **18,** 589–593.

Richter H. (1972) Wie entstehen Saugspannungsgradienten in Bäumen? *Berichte der Deutschen Botanischen Gesellschaft* **85,** 341–351.

Robson D.J. & Petty J.A. (1987) Freezing in conifer xylem I. Pressure changes and growth velocity of ice. *Journal of Experimental Botany* **38,** 1901–1908.

Robson D.J., McHardy W.J. & Petty J.A. (1988) Freezing in conifer xylem II. Pit aspiration and bubble formation. *Journal of Experimental Botany* **39,** 1617–1621.

Sperry J.S. & Robson D.J. (2001) Xylem cavitation and freezing in conifers. In *Conifer Cold Hardiness* (eds F.J. Bigras & S.J. Colombo), pp. 121–136. Kluwer Academic Publishers, Dordrecht, The Netherlands.

Sperry J.S. & Sullivan J.E.M. (1992) Xylem embolism in response to freeze-thaw cycles and water stress in ring-porous, diffuse-porous and conifer species. *Plant Physiology* **100,** 605–613.

Sperry J.S. & Tyree M.T. (1990) Water-stress-induced xylem embolism in three species of conifers. *Plant, Cell and Environment* **13,** 427–436.

Sperry J.S., Donnelly J.R. & Tyree M.T. (1988) A method for measuring hydraulic conductivity and embolism in xylem. *Plant, Cell and Environment* **11,** 35–40.

Spicer R. & Gartner B.L. (1998a) How does a gymnosperm branch (*Pseudotsuga menziesii*) assume the hydraulic status of a main stem when it takes over as leader? *Plant, Cell and Environment* **21,** 1063–1070.

Spicer R. & Gartner B.L. (1998b) Hydraulic properties of Douglas-fir (*Pseudotsuga menziesii*) branches and branch halves with reference to compression wood. *Tree Physiology* **18,** 777–784.

Spicer R. & Gartner B.L. (2001) The effects of cambial age and position within the stem on specific conductivity in Douglas-fir (*Pseudotsuga menziesii*) sapwood. *Trees* **15,** 222–229.

Spicer R. & Gartner B.L. (2002) Compression wood has little impact on the water relations of Douglas-fir (*Pseudotsuga menziesii*) seedlings despite a large effect on shoot hydraulic properties. *New Phytologist* **154,** 633–640.

Timell T.E. (1986) *Compression Wood in Gymnosperms*, Vol.1–3, 2150 pp. Springer-Verlag, Berlin, Germany.

Tyree M.T., Davis S.D. & Cochard H. (1994) Biophysical perspectives of xylem evolution: Is there a tradeoff of hydraulic efficiency for vulnerability to dysfunction? *IAWA Journal* **15,** 335–360.

Vogt U.K. (2001) Hydraulic vulnerability, vessel refilling, and seasonal courses of stem water potential of *Sorbus aucuparia* L. & *Sambucus nigra* L. *Journal of Experimental Botany* **52,** 1527–1536.

Wilson B.F. & Archer R.R. (1977) Reaction wood: induction and mechanical action. *Annual Review of Plant Physiology* **28,** 23–43.

Zimmermann M.H. (1978) Hydraulic architecture of some diffuse-porous trees. *Canadian Journal of Botany* **56,** 2286–2295.

Zimmermann M.H. (1983) *Xylem Structure and the Ascent of Sap*. Springer Verlag, Berlin, Germany.

Received 30 January 2003; received in revised form 17 March 2003; accepted for publication 25 March 2003